RSC Advances

PAPER

View Article Online
View Journal | View Issue

Cite this: *RSC Adv.*, 2024, **14**, 712

An innovative approach in titanium determination based on incorporating 2-amino-4-((4-nitrophenyl) diazenyl)pyridine-3-ol in a PVC membrane

R. F. Alshehri,[a] M. Hemdan,[b] A. O. Babalghith,[c] A. S. Amin *[d] and E. R. Darwish[e]

A pioneering optical sensor has been effectively developed to achieve precise and reliable detection of titanium ions. The sensor employs an optode membrane composed of 2-amino-4-((4-nitrophenyl) diazenyl)pyridine-3-ol (ANPDP) and sodium tetraphenylborate (NaTPB) incorporated into a plasticized PVC matrix, with dioctyl sebacate (DOS) acting as the plasticizer. When exposed to Ti^{4+} ions at pH 8.25, the color of the sensing membrane undergoes a distinctive transformation from yellow-orange to violet. Extensive investigations were carried out to assess and optimize various factors influencing the efficiency of ion uptake. Through careful experimentation, the optimum conditions were determined to be 60.0% DOS, 6.0% ANPDP, 30% PVC, and 4.0% NaTPB, with a rapid response time of 5.0 min. Within these conditions, the developed optode demonstrates an impressive linear range of 3.0–225 ng mL^{-1}, boasting detection (LOD) and quantification (LOQ) limits of 0.91 and 2.95 ng mL^{-1}, respectively. Moreover, the precision of the sensor, as indicated by the relative standard deviation (RSD%), remained consistently below 1.55% in six replicate determinations of 100 ng mL^{-1} Ti^{4+} across diverse membranes. The selectivity of the sensor was rigorously examined for a range of cations and anions, successfully establishing the tolerance limits for interfering species. Notably, the presence of EDTA as a masking agent did not compromise the high selectivity of the sensor. Consequently, the innovative probe holds significant potential as a reliable analytical tool for quantifying titanium content in various samples, including water, geological materials, soil, plants, paints, cosmetics, and plastics.

Received 1st October 2023
Accepted 14th December 2023

DOI: 10.1039/d3ra06679g

rsc.li/rsc-advances

Introduction

Titanium is considered an economically critical metal according to the 2023 United States Geological Survey.[1] Titanium occurs primarily in the minerals anatase, brookite, ilmenite, leucoxene, perovskite, rutile, and sphene. Of these minerals, only ilmenite, leucoxene, and rutile have significant economic importance. Titanium(IV) metal ions are prevalent in various sources, such as ores, volcanic materials, and even extraterrestrial substances, with significant implications in diverse fields including planetary science and chemistry.[2] Coordination complexes involving titanium play a crucial role in biological systems, catalysis, chemical synthesis, and numerous other applications.[3] The presence of Ti^{4+} ions in biomaterials, including implants, anticancer drugs, and imaging agents, raises the possibility of their involvement in metabolic pathways within biological systems.[4] However, despite their importance, the existing scientific literature provides limited information on the specific compounds formed by Ti^{4+} in biological chemistry. Furthermore, the poor solubility and limited bioavailability of these compounds suggest restricted hazardous effects *in vivo*.[5] Nonetheless, similar to aluminum (Al^{3+}), Ti^{4+} may present unforeseen challenges within the biosystem.[6]

The use of titanium in sectors such as cosmetics, food production, paint manufacturing, and sunscreen formulation, despite its advantages, poses a significant health risk.[7] It has been previously reported that children, particularly in the age group most exposed to titanium, encounter this element through the consumption of confectionery products.[8,9]

Titanium is widely present in plastics and polymers, as derivative compounds of Ti^{4+} are incorporated as fillers, additives, or colorants.[10] Moreover, titanium serves as a vital catalyst in polymerization reactions, exerting a significant influence on the oxidation and stability of plastics, thus underscoring the imperative to accurately determine the metallic content, particularly titanium, in order to assess the suitability of polymer applications.[11,12]

[a]*Chemistry Department, Faculty of Sciences, Taibah University, Kingdom of Saudi Arabia*
[b]*School of Biotechnology, Badr University in Cairo (BUC), Badr City, 11829, Cairo, Egypt*
[c]*Med. Genetics Dep., College of Medicine, Umm Al Qura University, Makkah, Saudi Arabia*
[d]*Chemistry Department, Faculty of Science, Benha University, Benha, Egypt. E-mail: asamin2005@hotmail.com*
[e]*Chemistry Department, Faculty of Science, Port Said University, Port Said, Egypt*

Comprehensive examination of food samples, encompassing vegetables, fruits, and fish meat, consistently reveals negligible or indiscernible levels of titanium.[9] However, it is noteworthy that cheese samples display significant concentrations of titanium, primarily as a result of the deliberate addition of titanium dioxide during the manufacturing process, specifically for renowned mozzarella cheese.[13] Moreover, the deliberate incorporation of titanium serves to augment the overall quality of cheese.[14]

Commonly employed techniques in control laboratories include flame emission spectrometry, inductively coupled plasma with atomic emission spectrometry (ICP-AES) with LODs of 4.0 μg L^{-1},[15,16] as well as, flame atomic absorption spectrometry (FAAS) using a nitrous oxide flame, which has a law detection limit (LOD) of 100 μg L^{-1}.[17] For enhanced sensitivity, alternative methods such as molecular spectrophotometry (MAS) utilizing sensitive reagents like chromotropic acid or pyridilazo resorcinol,[18] or Inductively Coupled Plasma Mass Spectrometry (ICP-MS) with a LOD of 0.06 μg L^{-1},[19–21] can be employed. Other approaches include adsorptive stripping voltammetry (AdSV),[22] reverse-phase high-performance liquid chromatography,[23] kinetic methods (such as flow kinetic spectrophotometry[24] and catalytic fluorimetry[25]), gravimetric filter weight (G/FW),[26] electrothermal atomic absorption spectrometry (ETAAS), sensor devices,[27,28] and chemiluminescence.[29] These characterization methods are expensive, so having low-cost, rapid alternative sensing technologies for metals prospecting and process monitoring during titanium production is very useful.

The application of X-ray fluorescence has proven to be effective in analyzing trace amounts of titanium in water samples.[30,31] This method enables the detection of cesium and titanium with sensitivities of approximately 0.4 μg kg^{-1} and 30 μg kg^{-1}, respectively, for both the ionic and particulate forms of these metals. Notably, titanium concentrations in seawater have been observed to range between 1.0 and 9.0 μg L^{-1}.[32] Additionally, Hamilton and Minski conducted a study utilizing spark-source mass spectroscopy to determine trace elements, including titanium, in water samples.[33]

Indeed, techniques such as X-ray fluorescence and spark-source mass spectroscopy can be costly due to the requirement for specialized equipment and skilled operators. As a result, spectrophotometry has emerged as one of the most widely employed detection methods. This method offers advantages such as rapid detection times, high precision, accuracy, and comparatively less expensive instrumentation. Spectrophotometry has thus gained popularity for Ti^{4+} analysis, providing a cost-effective alternative without compromising on performance.

While various methods have been reported for titanium determination, it is worth noting that sensor devices offer the advantage of simplicity and affordability. However, they may provide lower sensitivity compared to more sophisticated and expensive techniques.[34–40] Therefore, there is a need for increased research attention to develop accurate methods that combine selectivity and sensitivity for the determination of titanium concentration. By focusing on the development of such methods, researchers can address the existing limitations and pave the way for improved titanium analysis techniques.

The sensor is capable of real-time monitoring, that would also be an advantage over other techniques.[15–33] In the last three decades, there has been a substantial increase in interest in optical chemical sensors, commonly known as optodes or optrodes, as promising alternatives to electrochemical sensors.[41] Optodes offer several advantages, including lower detection limits and high sensitivity.[42] Furthermore, they leverage the spectral properties associated with the analyte or provide analyte-specific indications.[43] Unlike electrochemical sensors, optodes eliminate the need for internal or external reference devices, do not require extensive preconditioning time, and are immune to electrical noise interference.[44] These characteristics make optodes highly appealing for a broad range of applications in chemical sensing and analysis.

The selection of a suitable matrix for membrane optodes is guided by numerous factors. These include analyte permeability, cost-effectiveness, favorable mechanical characteristics, compatibility with ease of miniaturization, plasticization, and remote sensing, minimal sample manipulation requirements, and the capability to immobilize both the chromophore and extractant, as outlined in references.[45–47] Among the available options, polyvinyl chlorides (PVC) are widely used polymers in optical sensors. PVC possesses numerous advantageous properties and exhibits excellent performance compared to sol–gel matrices in most applications. Its transparency makes PVC polymers particularly suitable for optodes that employ visible spectrophotometric detection methods.[48] A plethora of optodes have been reported for the trace analysis of various analytes, including metal ions, anions, and organic compounds.[49–54]

2-Amino-4-((4-nitrophenyl)diazenyl)pyridine-3-ol (ANPDP) is an amorphous solid with a yellow-orange color, exhibiting excellent solubility in common organic solvents such as acetone, ethanol, and methanol. Previously, this reagent was utilized for spectrophotometric determination and its interaction with zinc at pH 9.0 using cloud point extraction in Triton X-114 at λ_{max} 605 nm.[55] In this study, we present a novel approach utilizing ANPDP in the development of a PVC sensor for the selective, sensitive, and rapid colorimetric determination of titanium in various sample types, including geological materials, water, plants, soil, paints, plastics, and cosmetics at different conditions. To our knowledge, there have been no previous reports in the literature regarding a spectrophotometric probe specifically designed for monitoring titanium ions. Therefore, this study presents the first reported instance of a probe developed for this purpose.

Experimental

Reagents

In this research, all chemicals employed were of analytical grade and procured from reputable chemical suppliers, including Merck (Darmstadt, Germany) and Fluka (Buchs, Switzerland). The chemicals employed encompassed sodium tetraphenylborate (NaTPB), *o*-nitrophenyl octyl ether (*o*-NPOE), high molecular weight polyvinyl chloride (PVC), dioctyl sebacate (DOS),

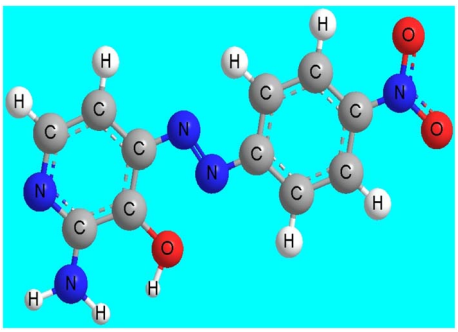

Scheme 1 The chemical structure of the synthesized ANPDP reagent.

dioctyl adipate (DOA), dibutyl phthalate (DBP), tributylphosphate (TBP), Na_2EDTA, and tetrahydrofuran (THF). To facilitate the experimental procedures, borate buffer solutions within a pH range of 6.5 to 9.5 were meticulously prepared.[56]

2-Amino-4-((4-nitrophenyl)diazenyl)pyridine-3-ol (ANPDP) was prepared according to the procedure described previously.[55] Characterization data to confirm the successful synthesis of ANPDP (*e.g.* mass spectra, NMR, and/or FTIR) is included.[55] The synthesized reagent's (ANPDP) chemical composition was identified as shown in the following Scheme 1.

A stock solution of Ti^{4+} ions at a concentration of 1×10^{-2} M (100 mL) is prepared by dissolving a precisely weighed quantity of titanium dioxide (TiO_2) with a molar mass of 79.86 g mol^{-1} in a concentrated sulphuric acid solution with careful heating. The resulting solution is then diluted to a final volume of 100 mL using distilled water. To ensure accuracy, the concentration of the Ti^{4+} stock solution is determined through a standardized procedure.[57]

Apparatus

The UV-vis spectrophotometer employed for evaluating spectra and measuring absorbance was a JASCO V 53 model manufactured in Tokyo, Japan. For the delivery of small volumes of the reagent metal, a Hamilton syringe with a capacity of 10 μL was utilized. All ICP-AES (Inductively Coupled Plasma-Atomic Emission Spectrometry) measurements were conducted using a PerkinElmer model 5300 DV instrument from Waltham, MA, USA. The pH of the solutions was ascertained using an Orion Research Model 601 A digital pH analyzer meter. The operating parameters were set as recommended by the manufacturer. Absorbance measurements were carried out by introducing the optical membrane sensor samples into a quartz cuvette. The absorbance of the optical membrane sensor samples was then measured relative to air and a blank optode sample. These reference points were utilized for comparison and calibration purposes, ensuring accurate and reliable absorbance measurements.

Membrane fabrication

The membrane was fabricated by thoroughly mixing specific quantities of the active components. Precisely, 45.0 mg of DOS constituting 60%, 22.5 mg of PVC constituting 30% of the membrane, 3.0 mg of NaTPB constituting 4.0%, and 4.5 mg of ANPDP constituting 6.0%, were combined in a glass vial. The components were dissolved in 2.0 mL of THF and vigorously agitated to achieve a uniform solution.

In preparation of the glass plate, a meticulous cleaning procedure was conducted using pure tetrahydrofuran (THF) to ensure the removal of any organic impurities present on the surface. The glass plate, measuring 1 mm × 9 mm × 50 mm, was carefully positioned within a spin-on device. Subsequently, a 100 μL volume of the previously prepared solution was injected onto the glass plate. The spin-on process was carried out for one minute at a rotation frequency of 750 rpm, ensuring uniform distribution of the solution. After the spin-on process, the membrane was exposed to the surrounding atmosphere and left to air-dry naturally for a few minutes, indicating the completion of the fabrication process.

Spectrophotometric methodology

The optode, fabricated and assembled, was carefully placed within a quartz cell having a path length of 1.0 cm. Subsequently, the quartz cell, containing the optode, was inserted into the spectrophotometer, which had been previously loaded with a test solution comprising ethylenediamine tetraacetic acid (EDTA) at a concentration of 2.0×10^{-2} M, and varying concentrations of Ti^{4+} ions. The pH of the solution was adjusted to 8.25. After an incubation period of 5.0 minutes to allow for equilibration (Scheme 2), the net absorbance of the optode was measured at a wavelength of 642 nm. The measurement was performed against a blank membrane, prepared in a similar manner but without the presence of Ti^{4+}, serving as a reference for comparison.

Stoichiometric ratio of the Ti^{4+}–ANPDP complex

The continuous-variation technique (Job's method) and molar ratio method, were used to determine the stoichiometry of the PIM–ANPDP complex. Both of which were run at pH 8.25 at Ti^{4+}

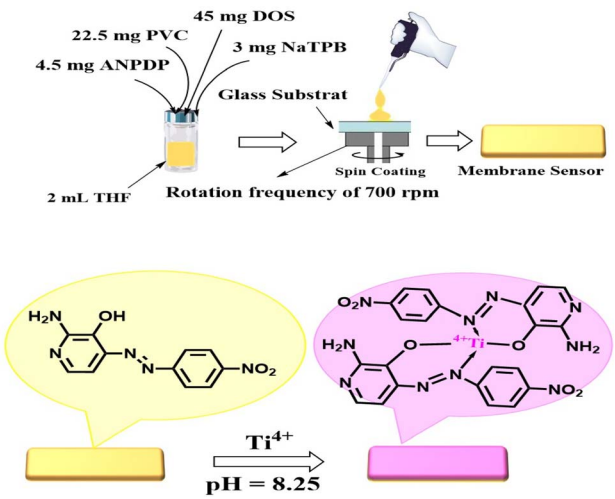

Scheme 2 Representative diagram for the sensing Ti^{4+} optode membrane.

and ANPDP concentrations of 5×10^{-3} M and at λ_{max} 567 nm. The molar ratio method was conducted using variable volumes of both ANPDP and Ti^{4+} (0.2–4.0 mL) of 5×10^{-3} M at pH 8.25 to prepared different ratio. The analysis was executed at the absorption maximum wavelength of 642 nm.

Digestion of samples

Water samples. In natural water environments, it is well-documented that titanium species predominantly exist in the form of TiO_2.[58] As a result, a digestion process is necessary to transform these titanium species into liberated Ti^{4+} ions, which are compatible with interaction within the prepared optode. To commence the digestion procedure as described in reference,[59] a comprehensive selection of water samples including river water, mineral water samples, tap water, and sea water were collected from various locations in Egypt. To remove any suspended solids present in the samples, a filtration step was employed using a membrane filter with a pore size of 0.45 μm. This filtration process ensured the removal of unwanted particulate matter, preparing the samples for further analysis.

The next step in the digestion procedure involved transferring 20 mL of each filtered sample into a porcelain crucible. The crucible was then placed in an environment with a temperature of 70 °C and left until the complete evaporation of the samples was achieved. This drying process ensured the removal of excess water content, preparing the samples for further processing. Following evaporation, 1.0 g of potassium peroxodisulfate ($K_2S_2O_8$) was introduced to the crucible containing the sample. The mixture was then fused using a Bunsen burner, allowing it to heat for approximately 15 min or until the generation of fumes ceased. Subsequently, the resulting residue was dissolved by adding 10 mL of a 0.1 M of nitric acid solution. The solution was thoroughly stirred on a hot plate set at approximately 90 °C for a minimum duration of 5.0 minutes. Finally, to achieve the desired concentration, each sample solution was diluted to a final volume of 25 mL using a 0.1 M HNO_3 solution. This preparation process ensured the samples were ready for subsequent analysis using the optode method at pH 8.25.

Geological samples analysis. Geological samples, comprising black sand sourced from the Mediterranean Coast in Egypt, wadi deposits collected from Marsa Alam in Egypt, as well as clay 1 from El-Sheikh Fadl and clay 2 from Gebel Qarara, both located in El-Minya Governorate, Egypt, were procured from the Geology Department within the Faculty of Science at Benha University. Prior to analysis, these samples were initially subjected to a crushing process and subsequently dried at a temperature of 100 °C for a duration of 2.0 hours.

To decompose the dried samples, 0.25 g of each sample was carefully transferred into a Teflon cup. Aqua regia was added in a volume of 5.0 mL. Caution: aqua regia is extremely toxic and corrosive, and should be handled in a fume hood only, using proper personal protection equipment, as well as guidance on safety precautions.[60] The mixture was then slowly heated until it reached near dryness. This step was repeated twice, with an additional 5.0 mL of aqua regia added each time to ensure thorough decomposition. The resulting residue was dissolved by adding 5.0 mL of concentrated hydrofluoric acid and heating the mixture until it reached near dryness. Subsequently, 2.0 mL of concentrated sulfuric acid (H_2SO_4) was added drop wise, and the mixture was further heated to remove any excess HF through volatilization.

To prepare the samples for analysis, the dissolved samples were diluted with double distilled water to a final volume of 100 mL in a volumetric flask. For further analysis, appropriate work solutions were prepared by diluting the prepared samples accordingly. This ensured that the samples were ready for accurate analysis using the desired analytical techniques after adjusted the pH to 8.25 with buffer solution.

Plant sample. To perform the sample analysis, a weight of the sample, specifically 100 g, was subjected to ashing in a porcelain crucible at a temperature of 450 °C for duration of 3.0 hours. Subsequently, 10 g of the obtained ash was transferred into a 200 mL Borosil beaker. In the beaker, the ash was digested in a sand bath by adding 100 mL of concentrated HCl and 20 mL of concentrated HNO_3. The digestion process was carried out for approximately 1.0 h. After the digestion process, the hot solution underwent centrifugation to separate any solid particles. The resulting supernatant, which contained the dissolved components of interest, was carefully decanted to remove any residual siliceous matter. The residue remaining after decantation was then subjected to boiling with 50 mL of 0.1 M HCl. This step aimed to further dissolve any remaining compounds and facilitate their extraction from the residue. The resulting mixture was subsequently filtered to remove any insoluble particles. The filtrate, along with the washings obtained during the filtration step, was then subjected to evaporation to remove excess solvent. The evaporation process led to the formation of a dry residue, which contained the analytes of interest. To prepare the sample for analysis, the dry residue was dissolved in a suitable solvent, and the resulting solution was accurately diluted to a final volume of 100 mL using 0.1 M HCl in a volumetric flask. This prepared solution was now ready for further analysis and determination of the desired analytes the pH achieved to 8.25 and determination of the desired analytes.

Determination of Ti^{4+} in paint

To analyze the paint sample, a weighed portion of the sample, specifically 2.5 g, is dissolved in ether. Subsequently, the dissolved sample is further dissolved in 5.0 mL of concentrated HCl with gentle heating for a few minutes. After the heating step, the aqueous layer is separated from the solution. The resulting solution is then diluted to a final volume of 25 mL using deionized water. From this diluted solution, a volume of 1.0 mL is withdrawn and mixed with tannic acid. The absorbance of the mixture is measured at a wavelength of 436 nm against a blank reference.

Quantification of titanium(IV) in a cosmetic (sunscreen) cream

To analyze the cream sample, a weighed portion of the sample, specifically 1.0 g, is dissolved in ether. Subsequently, the dissolved sample is further dissolved in 5.0 mL of a 0.1 M HCl solution with heating for 10 minutes. After the heating step, the

aqueous layer is separated from the solution. The resulting solution is then diluted to a final volume of 25 mL. From this diluted solution, a volume of 1.0 mL is taken and subjected to analysis using the proposed optode described earlier after adjusted the pH to 8.25. The absorbance of the sample is measured at a wavelength of 642 nm against a blank optode reference.

Plastic dissolution protocol

The plastic films made of polyethylene (PE) and polypropylene (PP) were washed and dried to eliminate any surface contaminants. They were subsequently cut into small pieces with a maximum size of less than 0.5 cm. Random sampling was employed to select the pieces for analysis, ensuring a representative sample. The selected pieces were weighed individually, with each sample weighing approximately 2.0 g. This significant sample quantity was chosen to minimize potential issues arising from inhomogeneous sampling. To initiate mineralization, 10 mL of concentrated H_2SO_4 was added to each sample, followed by oxidation using 10 mL of concentrated hydrogen peroxide (H_2O_2). The samples were heated in a Kjeldahl flask, maintaining an appropriate maximum temperature to facilitate the mineralization process. After mineralization, the resulting sample solutions were carefully evaporated to remove any excess solvent. Finally, the solutions were diluted to a final volume of 50 mL using de-ionized water in calibrated flasks. These prepared sample solutions are now ready for further analysis after adjusted pH to 8.25.

Results and discussion

Preliminary investigations

Through meticulous optimization of the fabrication process, a highly efficient sensor was developed by incorporating 2-amino-4-((4-nitrophenyl)diazenyl)pyridine-3-ol (ANPDP) and sodium tetraphenylborate (NaTPB) into a plasticized PVC membrane enriched with dioctyl sebacate (DOS). This novel configuration enabled the spectrophotometric determination of Ti^{4+} ions with remarkable precision. Upon diffusion of Ti^{4+} ions into the membrane, a captivating transformation occurred as ANPDP formed a complex, causing a striking shift in the membrane color from a vibrant yellow-orange to an alluring violet hue. The absorption spectra displayed in Fig. 1 eloquently depict the distinct profiles of the ANPDP in solution and membrane and its optodes when exposed to varying concentrations of Ti^{4+} ions. Notably, the membrane devoid of Ti^{4+} ions exhibited a prominent absorbance peak at 478 nm in solution. In stark contrast, the presence of Ti^{4+} ions induced a captivating modification, with the maximum absorbance shifting to a mesmerizing 642 nm. A meticulous comparison of the immobilized reagent and its complex spectra within the optode, as illustrated in Fig. 1, with their counterparts in solution, revealed compelling results. The immobilized reagent and the complex formed both exhibited bathochromic shifts of 20 nm and 35 nm, respectively, indicating a significant structural conformation difference compared to their solution

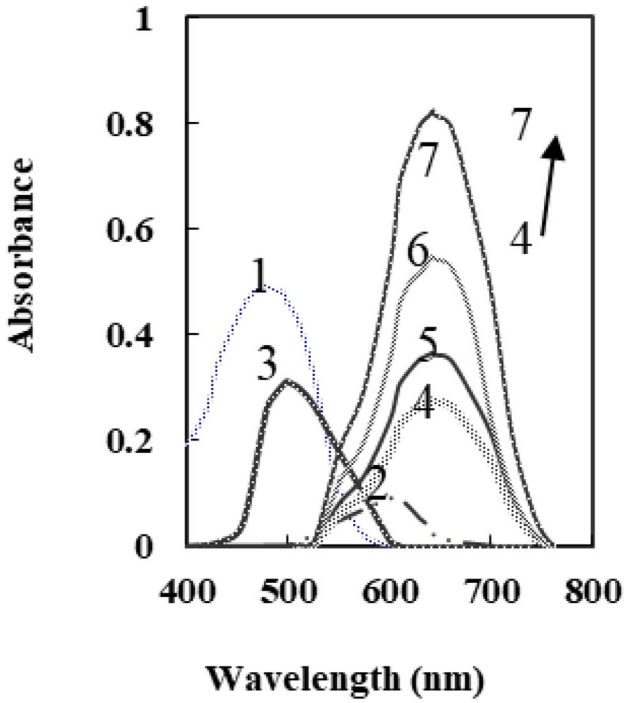

Fig. 1 Absorption spectra of (1) – R in solution; (2) – R–Ti in solution and (3) – R optode (4) – 7 R–Ti optode at 75, 100, 150 and 225 ng mL^{-1} at pH 8.25.

counterparts.[60] This suggests that the immobilized reagent adopts a more pronounced conformation, leading to enhanced interaction and complex formation with the target analyte. The observed bathochromic shifts reflect a shift towards longer wavelengths in the absorption spectra, highlighting the improved performance and sensitivity of the proposed system.

Intriguingly, the proposed optical sensor was found to operate as a remarkable probe, as the analytes mass transfer from the sample to the sensing layer demonstrated an intriguingly incomplete reversibility. This distinctive behavior further accentuates the sensor's exquisite sensitivity and its capability to unravel intricate analytical insights, surpassing conventional methodologies.[60]

Method optimization

To harness the full potential of the optode, it is imperative to meticulously optimize the quantities of its constituent ingredients and fine-tune the experimental conditions. In the pursuit of this optimization, a systematic one-at-a-time approach was adopted. The analytical signal was calculated by measuring the variance in absorbance at 642 nm between the optode membrane when exposed to 100 ng mL^{-1} of Ti^{4+} and when it was not exposed to Ti^{4+}. This differential absorbance served as the key indicator for evaluating the performance and efficacy of the optode under varying experimental parameters. By carefully analyzing and manipulating these factors, the optode can be honed to deliver optimal results and unlock its true analytical capabilities.

Influence of membrane composition

The performance and effective concentration range of each optode are heavily influenced by the selection of ingredients including the base matrix, solvent mediator, ionophore, and other additives incorporated into the membrane structure. Consequently, utmost importance lies in the careful selection of the optode matrix as the primary consideration. Through observation, it has been determined that high molecular weight PVC exhibits exceptional suitability as the membrane base. This choice is supported by several key factors, including its ability to maintain appropriate transmittance, enable secure fixation of ANPDP as the reagent without any risk of leakage, provide robust mechanical stability, and ensure reliable permeability to Ti^{4+} ions.

Achieving a homogeneous and cohesive organic phase is crucial in the preparation of the membrane, and this requires careful selection of solvent mediators or plasticizers that are compatible with the polymer used. In this particular study, various solvents such as DOS, DBP, DOA, *o*-NPOE, and TBP, were examined as potential plasticizers. Interestingly, as shown in Fig. 2a, *o*-NPOE and DOA demonstrated good sensitivity; however, membranes containing these plasticizers exhibited undesirable reagent leakage within short time periods. Conversely, the membrane incorporating DOS proved to be the most suitable choice, delivering optimal response and minimal ANPDP leakage from the membrane structure.

Based on the results displayed in Table 1, the membrane-based sensors incorporating a weight proportion of 2.0 for DOS to PVC demonstrated superior absorbance values. Therefore, 45.0 mg of DOS (60.0%) was identified as the optimal value for achieving optimal sensor performance.

In the proposed optical sensor, ANPDP plays a dual role as both the chromoionophore and ionophore. Therefore, it is imperative to fine-tune the amount of ANPDP within the composition of membrane. The influence of different ANPDP quantities on the membrane response is outlined in Table 1. As depicted, the absorbance increased as the ANPDP amount increased up to 4.5 mg, but started to decrease at higher concentrations due to membrane leakages. Consequently, 4.5 mg of ANPDP (6.0%) was determined as the optimal value for achieving the desired performance of the sensor.

The inclusion of an anionic additive, such as NaTPB, in the membrane has been found to enhance the ion–exchange equilibrium, resulting in complete mass transfer process of Ti^{4+} ions into the membrane and a reduction in response time.[61] Therefore, in subsequent investigations, the influence of NaTPB (3.0 mg) as an anionic additive was investigated with different plasticizers to evaluate its impact on membrane properties.

As depicted in Fig. 2b, the inclusion of NaTPB led to increased sensor responses but also caused reagent leakages from all the membranes. The amount of NaTPB was varied within the range of 1.0–5.0 mg, and the results are summarized in Table 1. The highest absorbance was observed when using 3.0 mg of NaTPB, indicating its significant contribution to the sensor response. At lower amounts, the absorbances decreased due to limited mass transfer of Ti^{4+}, resulting in lower analyte uptake. On the other hand, higher quantities of NaTPB led to the leakage of ANPDP from the membrane, causing a decline in absorbance. The ANPDP leakage percentage is measured quantitatively by decreasing the absorbance compared to the highest value. Based on these observations, an optimal amount

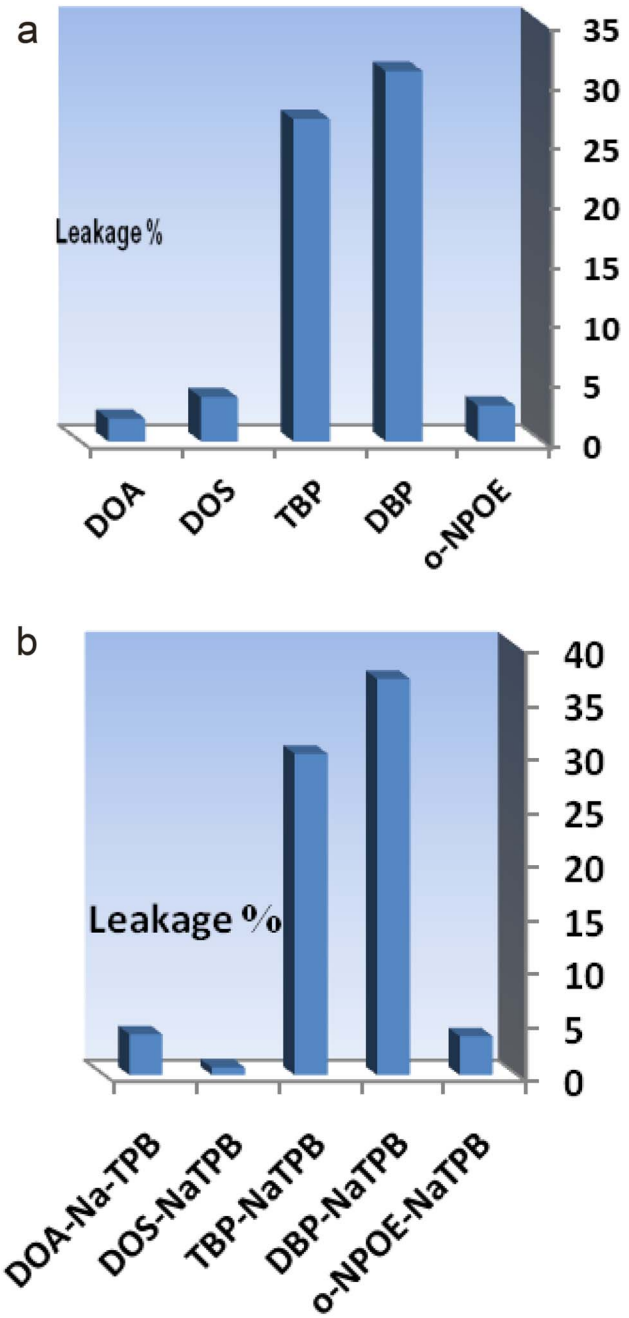

Fig. 2 (a) Effect of plasticizer nature on the response of the membrane leakage % after 5.0 min. Conditions: $[Ti^{4+}] = 100$ ng mL^{-1}; $T = 25$ °C; membrane layer contained 22.5 mg of PVC, 45.0 mg of each plasticizers, 4.5 mg ANPDP. (b) Illustrates the impact of varying anionic additives with different plasticizers on membrane leakage percentage after 5.0 min. The experimental conditions were as follows: $[Ti^{4+}] = 100$ ng mL^{-1}; temperature = 25 °C; the membrane layer consisted of 22.5 mg of PVC, 45.0 mg of each plasticizer, 4.5 mg ANPDP, and 3.0 mg of NaTPB.

Table 1 The impact of varying membrane compositions on the absorbance of the proposed optode, containing 100 ng mL^{-1} Ti^{4+}

Optode	PVC (mg)	DOS (mg)	ANPDP (mg)	NaTPB (mg)	Response time (min)	Absorbance[a] (642 nm)
1	22.5	35	4.5	3	5.0	0.246
2	22.5	40	4.5	3	5.0	0.317
3	22.5	45	4.5	3	5.0	0.365
4	22.5	50	4.5	3	5.0	0.326
5	22.5	55	4.5	3	5.0	0.289
6	22.5	45	2.0	3	5.0	0.172
7	22.5	45	4.0	3	5.0	0.325
8	22.5	45	6.0	3	5.0	0.346
9	22.5	45	8.0	3	5.0	0.309
10	22.5	45	10	3	5.0	0.273
11	22.5	45	4.5	1	5.0	0.212
12	22.5	45	4.5	2	5.0	0.318
13	22.5	45	4.5	3	5.0	0.366
14	22.5	45	4.5	4	5.0	0.323
15	22.5	45	4.5	5	5.0	0.276
16	22.5	45	4.5	3	2	0.258
17	22.5	45	4.5	3	4	0.327
18	22.5	45	4.5	3	6	0.366
19	22.5	45	4.5	3	8	0.365
20	22.5	45	4.5	3	10	0.364

[a] The mean absorbance ($n = 3$) of every parameter is recorded from three solutions of 100 ng mL^{-1} Ti^{4+} (pH 8.25).

of 3.0 mg of NaTPB (4.0%) was determined as the most effective concentration for incorporating into the composition of the membrane.

Impact of pH

The impact of pH fluctuations on the optodes response was investigated within a range of 6.5 to 10.5. As illustrated in Fig. 3, the optodes absorbance reached its peak at pH 8.25. The diminished response at the lower pH may be explained by the extraction of H^+ from the test solution into the membrane, *via* protonation of the nitrogen atom of ANPDP, resulting in an expected change in the formation of a complex. On the other hand, at pH values higher than 8.25, hydrolysis of Ti^{4+} ions occurs, leading to the formation of hydroxide species such as $[Ti(OH)_2]^{2-}$. This phenomenon likely hinders the complete diffusion of Ti^{4+} ions into the membrane. Based on these findings, a buffer solution with a pH of 8.25 was selected as the preferred choice for all experimental procedures.

Stoichiometry of Ti^{4+}–ANPDP complex

The Ti^{4+}–ANPDP complex stoichiometry was determined using Job's technique and the molar ratio process. First, as shown in Fig. 1, the absorption spectra of ANPDP and the Ti^{4+}–ANPDP complex were obtained. As seen in this figure, the highest absorption of ANPDP is 478 nm, whereas the greatest absorption peak of the Ti^{4+}–ANPDP complex was detected at 607 nm. The two procedures were then performed at 607 nm, which is the wavelength at which the complex exhibits the maximum absorbance. The plot of absorbance against the Ti^{4+} mole fraction produced by changing the ANPDP and Ti^{4+} concentrations revealed an inflection at 0.35, indicating the presence of two ANPDP molecule in the established complex. Furthermore, the plot of absorbance *versus* the molar ratio of ANPDP to Ti^{4+}, obtained by varying the ANPDP concentration, showed inflection at molar ratio 2.0, indicating presence of two ANPDP molecules in the formed complex. As a consequence, the stoichiometric ratio was revealed to be (2 : 1) [ANPDP : Ti^{4+}] as

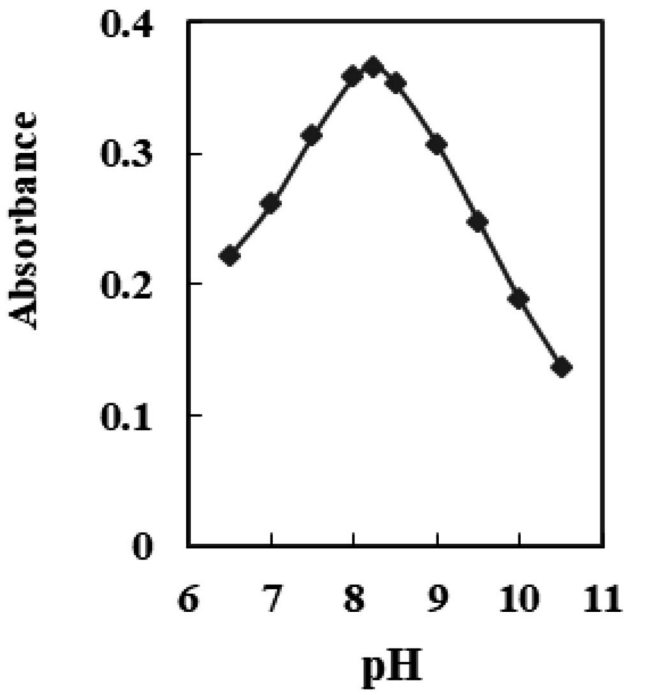

Fig. 3 Effect of pH on the absorbance of the proposed optode; conditions: [Ti^{4+}] = 100 ng mL^{-1}; $T = 25$ °C; response time = 5.0 min; membrane layer contained 22.5 mg of PVC, 45.0 mg DOS, 4.5 mg ANPDP and 3.0 mg NaTPB.

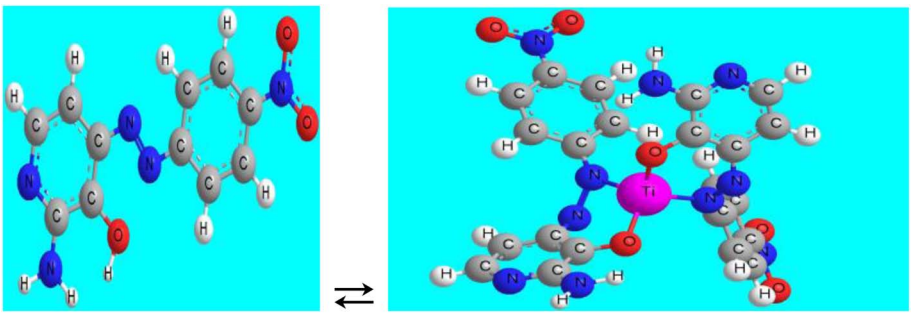

Scheme 3 The suggested chemical structure of the Ti^{4+}–ANPDP complex.

represented in Scheme 3. The conditional formation constant ($\log K$) was determined to be 8.35; however, the true constant was 8.20, employing the Harvey and Manning equation, and the data provided from the previous techniques. The mechanism of formation of the complex is represented in Scheme 2 as:

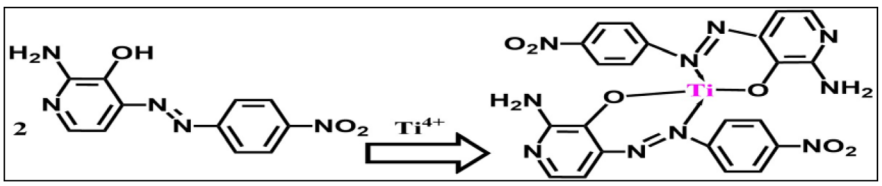

Influence of time

The time taken for the optodes to respond is determined by the rate at which Ti^{4+} ions diffuse from the solution into the membrane, representing the slowest step in the complexation process. In order to evaluate the impact of this parameter on the optode response, a range of 2 to 10 minutes was examined. The results depicted in Table 1 reveal that a minimum time span of 5.0 minutes is necessary to achieve complete uptake of Ti^{4+} ions at room temperature. Notably, it was observed that the absorbance of the membrane remained consistent for a duration exceeding 90 min, indicating the long-term stability and reliability of the optode. These findings underscore the meticulous optimization of the optode design to ensure accurate and robust performance.

Properties of membrane

The characteristics of the optode were evaluated by measuring absorbance changes at 642 nm using individual solutions containing 75, 100, 150, and 225 ng mL^{-1} of Ti^{4+}. As depicted in Fig. 1, the optodes exhibited a 95% response within 5.0 minutes for all four concentration levels. The stability of the membranes was assessed over a 90 min period, during which the mean difference in absorbances for the mentioned solutions was ± 0.016, indicating minimal variation. Furthermore, the membrane responses remained stable for one month when stored in ambient air.

The rejuvenation of the suggested optode membrane was investigated using various reagents, including HNO_3, NaF, HCl, and oxalic acid, at different concentrations. However, none of these reagents were capable of thoroughly regenerating the optode membrane. Hence, the membrane can serve as a trustworthy sensor for the quantification of titanium ions, as it retains its functionality even following exposure to test solutions.

Analytical characteristics

Table 2 provides an overview of the analytical properties of the optimized membrane, encompassing the regression equation, reproducibility, linear range, quantification limit and detection limit[62] for the determination of titanium. The limit of detection, calculated as $C_L = 3S_B/m$ (where C_L represents the limit of detection, S_B denotes the standard deviation of the blank, and m signifies the slope of the calibration equation), was determined to be 0.91 ng mL^{-1}. Additionally, the relative standard deviation (RSD%) for six replicate determinations of 100 ng mL^{-1} Ti^{4+} using various membranes was found to be 1.55%. This outcome signifies that the responses obtained from the fabricated membranes exhibit good reproducibility, and no significant differences were observed among the individual measurements conducted throughout the experiments.

To gauge the precision and accuracy of the suggested method, solutions containing three distinct concentrations of Ti^{4+} were prepared. The assay process was conducted in six replicates, and the relative standard deviation (RSD%) was computed to assess repeatability (intra-assay) within the same day and over five different days to evaluate intermediate precision (inter-assay). The analytical outcomes acquired for intra-day and inter-day precision and accuracy substantiate that the proposed procedure displays commendable repeatability and reproducibility.

The comprehensive comparative analysis conducted between our proposed method and existing methodologies has unequivocally established the exceptional performance of our

Table 2 Analytical properties of the presented optical sensor

Parameters	Proposed optode	Parameters	Proposed optode
pH	8.25	Quantification limit (ng mL^{-1})	2.95
λ_{max} (nm)	642	Reproducibility (RSD%)[a]	1.55
Beer's range (ng mL^{-1})	3.0–225	Regression equation	
Ringbom range (ng mL^{-1})	10–205	Slope (ng mL^{-1})	22.8
Molar absorptivity (L mol^{-1} cm^{-1})	1.74×10^6	Intercept	−0.07
Detection limit (ng mL^{-1})	0.91	Correlation coefficient (r)	0.9988

[a] For six replicate determination of 100 ng mL^{-1} Ti^{4+}.

Table 3 An overview of spectrophotometric techniques demonstrating the benefits of the suggested method

Reagent	λ_{max} [nm]	Remarks	$\varepsilon \times 10^4$ (L mol^{-1} cm^{-1})	LOD (μg mL^{-1})	Ref.
2,4-Dihydroxybenzaldehyde isonicotinoyl hydrazone	430 500	Narrow Beer's law range	1.35	0.030	63
N-Phenyllaurohydroxamic acid and phenylflurone	540	Involves an extraction step	2.33	—	64
Mixed-ligand titanium(IV)-fluoride-alizarin complex	513	Involves extraction step; narrow Beer's law range	7.0	—	65
Cetyltrimethylammonium, cetyl-pyridinium or tetradecyldimethyl benzylammonium cation	420	Involves an extraction step	(6–7)	0.006	66
N^1-Hydroxy-N^1,N^2-diphenyl-benzamidine and thiocyanate	400	Involves extraction step; narrow Beer's law range	2.0	0.060	67
N′-(2-Hydroxybenzylidene)-3-oxobutanehydrazide	500	Involves extraction step; narrow Beer's law range	1.68	—	68
2,6,7-Trihydroxylphenylfluorone derivatives, nitrilotriacetic acid and cetyltrimethyl ammonium bromide	576	Involves the formation of a quaternary complex	19	0.060	69
Thiocyanate and cetyltrimethyl ammonium bromide	421	Involves an extraction step	11–10	0.400	70
2,3-Dihydroxynaphthalene	375	Involves extraction and reextraction	3.2	0.600	71
3-Hydroxy-2-methyl-1-(4-tolyl)-4-pyridone	355	Involves extraction step; narrow Beer's law range	1.6	0.150	72
Chlorpromazine hydrochloride	417	Involves extraction step; narrow Beer's law range	2.6	0.060	73
N-Pivaloyl-*p*-chlorophenyl hydroxylamine	380	Involves an extraction step	0.53	—	74
BTAHQ using DLLME	626	Involves extraction step	40.4	0.220	75
ANPDP optode	642	No extraction step	174	0.0009	This work

approach. Our method showcases remarkable sensitivity, rapidity, and simplicity, surpassing the techniques described in the literature, as evidenced by the compelling results presented in Table 3. Notably, the achieved molar absorptivity surpasses that of previously reported methods.[63–75] underscoring the superior performance of our approach. Moreover, our procedure exhibits outstanding selectivity, characterized by impressively low limits of detection and quantification. When considering sensitivity and selectivity, our developed probe emerges as a clear frontrunner, offering distinct advantages over alternative approaches. It is important to highlight that our study represents a pioneering contribution by successfully employing ANPDP as an ionophoric reagent for optode preconcentration and determination of Ti^{4+} ions, thus introducing a novel and innovative aspect to the field.

Interferences

The specificity of the proposed optode was comprehensively evaluated by investigating the impact of common ions found in water samples on the determination of Ti^{4+} at a concentration of 100 ng mL^{-1}, under the optimized conditions. Various cations that could potentially be absorbed by the membrane or interact with Ti^{4+} ions, thereby impeding diffusion efficiency, were examined as potential interferences. The results, as summarized in Table 4, reveal that alkaline metals and anions such as nitrate, sulfate, chloride, and others exhibited no detrimental effects on Ti^{4+} uptake. Additionally, bivalent and select trivalent cations displayed no interference with the determination of Ti^{4+} at different ratios.

To address these interferences, EDTA was selected as a masking agent. The influence of EDTA on the determination of Ti^{4+} was investigated, and it was observed that $EDTA^{2-}$ did not significantly affect Ti^{4+} determination, causing less than a 3.5% negative deviation, unless present in a molar ratio exceeding 400-fold that of Ti^{4+} ions. Thus, the inclusion of EDTA (2.0×10^{-2} M) in the test solution effectively masks interfering cations, such as W(VI), Mo(VI), and Zr(IV), at a concentration of 500 ng mL^{-1}. Consequently, the proposed membrane sensor

Table 4 Tolerance ratios of diverse ions on the determination of 100 ng mL^{-1} of Ti^{4+}

Ion	Tolerance ratio
Borate, borax, benzoate	20 000
CH_3COO^-, NO_3^-, SO_4^{2-}, Cl^-	16 000
PO_4^{3+}, I^-, Br^-	15 000
Na^+, K^+, Ca^{2+}	12 500
Cu^{2+}, Co^{2+}, Mn^{2+}	10 000
Ni^{2+}, Pb^{2+}, Al^{3+}	8750
Ce^{3+}, Zn^{2+}, Mg^{2+}	6500
Mg^{2+}, Sr^{2+}, Cd^{2+}	5750
As^{3+}, Fe^{2+}, Fe^{3+}	5000
Cr^{3+}, Ag^+, Au^{3+}	3500
Pd^{2+}, Nb^{5+}	2500
V^{5+}, Sn^{2+}, Y^{3+}	1500
MoO_4^{2-}, WO_4^{2-}, Zr^{4+a}	500

[a] ≤5.0% Deviation in the presence of EDTA (2.0×10^{-2} M).

demonstrates excellent selectivity for monitoring Ti^{4+} in water samples.

Analytical application

To assess the reliability and accuracy of the proposed procedure, a series of experiments was conducted to determine Ti(IV) in spiked water samples (Table 5) as well as four real geological samples (Table 6). The results obtained from both ICP-AES and optode measurements demonstrated high accuracy, with a recovery rate exceeding 98.4%.

Furthermore, the information acquired from the examination of the geological samples were compared to the results obtained from solid XRF analysis (Table 6). Statistical analysis was performed using *t*-test and *F*-test approaches at a 95% confidence level with a sample size of $n = 5$.[76] The calculated values were found to be lower than the tabulated values, indicating that there was no significant difference between the two standard deviations at a 95% confidence level for both procedures.

These findings confirm that the proposed procedure is reliable and provides accurate results for the determination of Ti(IV) in various sample types, including spiked water samples and real geological samples.

In order to evaluate the accuracy and suitability of the proposed method for the analysis of real soil and plant samples, samples obtained from the industrial area of Shoubra were analyzed. Matrix interference was evaluated by comparing the slopes of calibration graphs with those obtained using the standard addition method. The results of the analysis are presented in Table 6. In addition, the determination of titanium in real plastic bags, which had varying titanium content and were made of polyethylene (PE) and polypropylene (PP), was performed using the new optode method. The same samples were also subjected to analysis using ICP-AES with robust conditions as recommended by the manufacturer and pneumatic

Table 5 Quantification of titanium in water samples using the optode and ICP–AES technique

Sample	Ti(IV) added (ng mL^{-1})	Optode method		ICP–AES method	
		Found[a] (ng mL^{-1})	Recovery (%)	Found[a] (ng mL^{-1})	Recovery (%)
Tap water	0.0	n.d[b]	—	n.d[b]	
	50	50.4 ± 0.43	100.80	49.1 ± 0.59	98.20
	100	99.5 ± 0.65	99.50	100.9 ± 0.76	100.90
	150	151.3 ± 0.80	100.87	152.2 ± 0.89	101.47
Well water	0.0	n.d[b]	—	n.d[b]	
	40	39.6 ± 0.44	99.00	40.6 ± 0.71	101.50
	80	80.7 ± 0.57	100.88	78.9 ± 0.80	98.63
	120	118.8 ± 0.78	99.00	123.0 ± 0.97	102.50
Polluted water	0.0	6.0		5.9	
	60	67.2 ± 0.59	101.82	65.1 ± 0.39	98.79
	120	125.2 ± 0.71	99.37	127.5 ± 0.56	101.27
	180	188.5 ± 0.85	101.34	182.4 ± 0.68	98.12
Sea water	0.0	0.9	—	1.00	—
	30	31.1 ± 0.64	100.65	30.5 ± 0.47	98.39
	60	60.5 ± 0.55	99.34	61.8 ± 0.78	101.31
	90	90.2 ± 0.38	99.23	89.7 ± 0.91	98.57
River water	0.0	n.d[b]	—	n.d[b]	—
	70	71.3 ± 0.72	101.86	69.4 ± 0.79	99.14
	140	138.2 ± 0.54	98.71	142.6 ± 0.39	101.47
	210	208.4 ± 0.43	99.24	214.5 ± 0.54	102.14
Mineral water	0.0	n.d[b]	—	n.d[b]	—
	25	25.3 ± 0.36	101.20	24.4 ± 0.67	97.60
	50	49.2 ± 0.63	98.40	51.1 ± 0.92	102.02
	75	75.8 ± 0.47	101.07	74.1 ± 0.59	98.80

[a] Mean ± SD ($n = 5$). [b] Not detected.

Table 6 Analytical findings of TiO_2 analysis in geological, soil and plant samples

	TiO_2[a] (wt%)				
Samples	XRF	ICP-OES[d]	Optode	*t*-Test[b]	*F*-Test[c]
Clay 1	0.31	0.32 ± 0.02 (3.42)	0.31 ± 0.01 (1.26)	1.12	2.21
Clay 2	1.15	1.17 ± 0.03 (2.84)	1.14 ± 0.04 (1.50)	1.31	2.78
Black sand	44.38	44.78 ± 1.05 (2.56)	45.28 ± 1.22 (2.49)	1.18	2.44
Wadi deposits	1.05	1.03 ± 0.05 (2.42)	1.04 ± 0.06 (2.12)	1.63	3.17
Soil sample (mg)		7.52 ± 0.05 (3.27)	7.50 ± 0.02 (1.86)	1.44	3.54
Pulp and paper		63.33 ± 0.05 (2.98)	63.56 ± 0.07 (1.42)	1.21	2.79
Paint and pigment		190.82 ± 0.05 (3.41)	190.87 ± 0.08 (1.56)	1.83	3.74

[a] TiO_2 was determined from Ti(IV). [b] *t*-Test between XRF and optode for five degrees of freedom at *P* (0.95) is 2.57. [c] *F*-Test between ICP-OES and optode measurements at *P* (0.95) is 5.05. [d] The results are the mean of five measurements ± SD (RSD%).

Table 7 Ti content on plastic films analyzed by proposed optode and ICP-AES as reference method

		Optode method		ICP–AES method			
Plastic type	Ti(IV) added (mg g^{-1})	Found[a] (mg g^{-1})	Recovery (%)	Found[a] (mg g^{-1})	Recovery (%)	*t*-Test[b]	*F*-Test[c]
Low content (PP)	0.0	0.8 ± 0.06	—	0.8			
	0.5	1.33 ± 0.43	102.31	1.22 ± 0.59	93.85	1.67	
	1.0	1.75 ± 0.65	97.22	1.88 ± 0.76	104.44		3.83
	1.5	2.35 ± 0.80	102.17	2.20 ± 0.89	95.65	1.82	
Medium content (PP)	0.0	12.5	—	12.4			
	3.0	15.46 ± 0.44	99.74	15.52 ± 0.71	100.78		2.68
	6.0	18.60 ± 0.57	100.54	18.15 ± 0.80	98.64	1.46	
	9.0	21.35 ± 0.78	99.30	21.60 ± 0.97	100.93		3.34
High content (PP)	0.0	26.00		25.90			
	5.0	31.15 ± 0.59	100.48	30.65 ± 0.39	99.19	1.08	
	10.0	35.75 ± 0.71	99.31	36.55 ± 0.56	101.81		2.63
	15.0	41.45 ± 0.85	101.10	40.55 ± 0.68	99.14	1.27	
Low content (PE)	0.0	0.50	—	0.50	—		
	2.0	2.55 ± 0.64	102.00	2.35 ± 0.47	94.00		2.95
	4.0	4.50 ± 0.55	100.00	4.75 ± 0.78	105.55	1.76	
	6.0	6.40 ± 0.38	98.46	6.70 ± 0.91	103.08		3.54
Medium content (PE)	0.0	12.0	—	12.1	—		
	8.0	20.3 ± 0.72	101.50	20.05 ± 0.79	99.75	1.31	
	16.0	28.35 ± 0.54	101.25	26.60 ± 0.39	94.66		2.79
	24.0	35.4 ± 0.43	98.33	36.65 ± 0.54	101.53	1.64	
High content (PE)	0.0	32.00	—	31.80	—		
	10.0	42.30 ± 0.36	100.71	31.45 ± 0.67	98.90		3.48
	20.0	51.25 ± 0.63	98.56	50.90 ± 0.92	98.26	1.55	
	30.0	61.15 ± 0.47	98.63	62.45 ± 0.59	101.55		2.96

[a] Mean ± SD ($n = 5$). [b] Not detected. [c] Results average of six consecutive measurements, paired *t*-test found value = 1.51; table value = 2.56 for 95% confidence level.

nebulization. The method's performance was assessed through spike addition experiments to determine its recovery. The significant findings from these experiments are summarized in Table 7. These results demonstrate the accuracy and reliability of the proposed method for the analysis of real soil, plant, and plastic bag samples, making it a valuable tool for titanium determination in various environmental matrices.

Conclusion

The introduced probe stands out as a precise, cost-effective, sensitive, and highly selective tool for titanium determination, using a PVC membrane combined with spectrophotometric analysis. Moreover, this proposed optode combines speed and simplicity with a broad dynamic range, consistent reproducibility, and an impressive limit of detection. In this research, the use of EDTA as a masking agent for Mo^{6+}, W^{6+}, and Zr^{4+} ions further enhances the method's selectivity. A comparative analysis between the suggested optode and previously documented techniques for titanium determination (as shown in Table 3) reveals that our approach, apart from being rapid and straightforward, offers comparable molar absorptivity and detection limits in comparison to some other methods. It is noteworthy that this technique, which marks its inaugural

usage in this study, has not been previously reported in the literature for titanium determination. The attained results underscore the precision and dependability of our proposed method when applied to real soil, plant, and plastic bag samples. This method proves to be a valuable instrument for titanium assessment across various environmental matrices, delivering heightened accuracy and practicality.

Author contributions

Reem Alshehri and Mohamed Hemdan: conceptualization, data curation, investigation, methodology, visualization, validation, writing – original draft, writing – review & editing. Ahmad Babalghith and Alaa Amin: conceptualization, methodology, data curation, investigation, supervision, validation, writing – original draft, writing – review & editing. Eman Darwish: conceptualization, investigation, methodology, validation, writing – original draft, writing – review & editing.

Conflicts of interest

The authors declare that they have no known competing financial interests or personal relationships that could have appeared to impudence the work reported.

Acknowledgements

The authors extend their appreciation to the Deputyship for Research & Innovation, Ministry of Education in Saudi Arabia for funding this research work through the project number 445-9-393. The authors' sincere thanks are due to Benha, and Port Said Universities, for providing the necessary facilities.

References

1 K. Szaciłowski, W. Macyk, A. D. Matuszek, M. Brindell and G. Stochel, *Chem. Rev.*, 2005, **105**, 2647–2694.
2 H. Cao, S. Liu and X. Wang, *Green Chem. Eng.*, 2022, **3**, 111–124.
3 A. L. Vavere and M. J. Welch, *J. Nucl. Med.*, 2005, **46**, 683–690.
4 C. Rey, C. Combes, C. Drouet, H. Sfihi and A. Barroug, *Mater. Sci. Eng., C*, 2007, **27**, 198–205.
5 C. Exley, *J. Inorg. Biochem.*, 2003, **97**, 1–7.
6 M. Geetha, A. K. Singh, R. Asokamani and A. K. Gogia, *Prog. Mater. Sci.*, 2009, **54**, 397–425.
7 J. Wang, Y. Liu, F. Jiao, F. Lao, W. Li, Y. Gu, *et al.*, *Toxicology*, 2008, **254**, 82–90.
8 L. Fabricius, Human exposure assessment of engineered inorganic nano-particles in food, Master thesis, Institute for fysikk, 2011, issue date 2011.
9 A. Weir, P. Westerhoff, L. Fabricius, K. Hristovski and N. von Goetz, *Environ. Sci. Technol.*, 2012, **46**, 2242–2250.
10 N. Allen, H. Khatami and F. Thompson, *Eur. Polym. J.*, 1992, **18**, 817–822.
11 L. Finelli, C. Lorenzetti, M. Messori, L. Sisti and M. Vannini, *J. Appl. Polym. Sci.*, 2004, **92**, 1887–1892.
12 K. Bichinhoa, G. Piresb, F. Stedileb, J. dos Santo and C. Wolf, *Spectrochim. Acta, Part B*, 2005, **60**, 599–604.
13 M. C. Lomer, R. P. Thompson, J. Commisso, C. L. Keen and J. J. Powell, *Analyst*, 2000, **125**, 2339–2343.
14 F. V. Kosikowski and D. P. Brown, *J. Dairy Sci.*, 1969, **52**, 968–970.
15 Y. K. Agrawal and S. Sudhakar, *Talanta*, 2002, **57**, 97–104.
16 R. K. Winge, V. J. Peterson and V. Fassel, *Appl. Spectrosc.*, 1979, **33**, 206–219.
17 G. F. Kirkbright and M. Sargent, *Atomic Absorption and Fluorescence Spectroscopy*, Academic Press, London, 1974.
18 Z. Marczenko, *Separation and Spectrophotometric Determination of Elements*, Ellis Horwood Ltd, New York, 1986.
19 A. Montaser and D. W. Golightly, *Inductively Coupled Plasmas in Analytical Atomic Spectrometry*, VCH, Weinheim, 1987.
20 K. Ra and H. Kitagawa, *J. Anal. At. Spectrom.*, 2007, **22**, 817–821.
21 J.-H. Lim, D. Bae and A. Fong, *J. Agric. Food Chem.*, 2018, **66**, 13533–13540.
22 J. Schmidt and W. Vogelsberger, *J. Solution Chem.*, 2009, **38**, 1267–1282.
23 Y. Nagaosa and S.-I. Segawa, *J. High Resolut. Chromatogr.*, 1994, **17**, 770–772.
24 J. Wang and R. He, *Anal. Chim. Acta*, 1993, **276**, 419–424.
25 F. Lazaro, M. D. Luque de Castro and M. Valcarcel, *Anal. Lett.*, 1985, **18**, 1209–1220.
26 S. C. Shome, *Analyst*, 1950, **75**, 27–32.
27 S. Ahmadzadeh, M. Rezayi, E. Faghih-Mirzaei, M. Yoosefi and A. Kassime, *Electrochim. Acta*, 2015, **178**, 580–589.
28 R. Tabaraki and F. Hajisharifi, *Chem. Pap.*, 2023, **77**, 2625–2633.
29 A. Tahirovic, A. Copra, E. O. Miklicanin and K. Kalcher, *Talanta*, 2007, **72**, 1378–1385.
30 D. Blagojevic, D. Lazic, D. Keselj, G. Ostojic and M. Imamovic, *Acta Chim. Slov.*, 2018, **65**, 380–387.
31 M. Blasius, S. Kerkhoff, R. Wright and C. Cothern, *J. Am. Water Resour. Assoc.*, 1972, **8**, 704–714.
32 H. Wake, H. Takahashi, T. Takimoto, H. Takayanagi, K. Ozawa, H. Kadoi, *et al.*, *Biotechnol. Bioeng.*, 2006, **95**, 468–473.
33 E. Hamilton and M. Minski, *Environ. Lett.*, 1972, **3**, 53–71.
34 I. M. I. Moustafa, A. S. Amin and E. R. Darwish, *RSC Adv.*, 2022, **12**, 26090–26098.
35 A. S. Amin, H. H. El-Feky and N. Hassan, *RSC Adv.*, 2022, **12**, 26620–26629.
36 H. H. El-Feky, A. S. Amin and E. M. I. Moustafa, *RSC Adv.*, 2022, **12**, 18431–18440.
37 E. M. I. Moustafa, A. S. Amin and M. A. El-Attar, *Anal. Biochem.*, 2022, **645**, 114835.
38 A. S. Amin, S. El-Bahy and H. H. El-Feky, *Anal. Biochem.*, 2022, **643**, 114579.
39 H. H. El-Feky, S. El-Bahy and A. S. Amin, *Anal. Biochem.*, 2022, **651**, 114720.
40 Z. Al-Mallah and A. S. Amin, *J. Ind. Eng. Chem.*, 2018, **63**, 281–287.

41 M. R. Ganjali, M. Hosseini, M. Hariri, F. Faridbod and P. Norouzi, *Sens. Actuators, B*, 2009, **142**, 90–96.
42 W. R. Seitz, in *Optical Ion Sensing Fiber Optic Chemical Sensors Biosensors II*, ed. O.S. Wolfbeis, CRC Press, Bocaraton, FL, 1991, pp. 1–19.
43 M. Shamsipur, M. Sadeghi, K. Alizadeh, H. Sharghi and R. Khalifeh, *Anal. Chim. Acta*, 2008, **630**, 57–66.
44 G. Absalan, M. Asadi, S. Kamran, S. Torabi and L. Sheikhian, *Sens. Actuators, B*, 2010, **147**, 31–36.
45 Y. Kalyan, A. K. Pandey, P. R. Bhagat, R. Acharya, V. Natarajan, G. R. K. Naidu and A. V. R. Reddy, *J. Hazard. Mater.*, 2009, **166**, 377–382.
46 M. R. Ganjali, R. Zare-Dorabei and P. Norouzi, *Sens. Actuators, B*, 2009, **143**, 233–238.
47 Y. Kalyan, A. K. Pandey, G. R. K. Naidu and A. V. R. Reddy, *Spectrochim. Acta, Part A*, 2009, **74**, 1235–1241.
48 S. Rastegarzadeh, N. Pourreza and I. Saeedi, *J. Hazard. Mater.*, 2010, **173**, 110–114.
49 A. Safavi and M. Bagheri, *Sens. Actuators, B*, 2004, **99**, 608–612.
50 M. K. Mahani, F. Divsar, M. Chaloosi, M. Ghanadi Maragheh, A. R. Khanchi and M. K. Rofouei, *Sens. Actuators, B*, 2008, **133**, 632–637.
51 S. Rastegarzadeh, N. Pourreza and I. Saeedi, *Talanta*, 2009, **77**, 1032–1036.
52 A. A. Ensafi, A. Katiraeifar and S. Meghdadi, *J. Hazard. Mater.*, 2009, **172**, 1069–1075.
53 M. Shamsipur, M. Sadeghi, K. Alizadeh, A. Bencini, B. Valtancoli, A. Garaud and V. Lippolis, *Talanta*, 2010, **80**, 2023–2033.
54 M. M. F. Choi, K. O. P. Chung and X. Wu, *Talanta*, 2002, **56**, 1027–1038.
55 A. H. Moustafa, H. A. El Sayed, A. S. Amin, A. M. El-Haggar and A. A. Gouda, *Egypt. J. Chem.*, 2023, **66**, 553–562.
56 H. T. S. Britton, *Hydrogen Ions*, Chapman and Hall, London, 4th edn, 1952.
57 A. I. Vogel, *Text Book of Quantitative Inorganic Analysis*, Pearson Education, Singapore, 6th edn, 2002.
58 R. N. M. J. Páscoa, I. V. Tóth, A. A. Almeida and A. O. S. S. Rangel, *Sens. Actuators, B*, 2011, **157**, 51–56.
59 D. Sánchez-Quiles, A. Tovar-Sánchez and B. Horstkotte, *Mar. Pollut. Bull.*, 2013, **76**, 89–94.
60 A. Safavi and M. Bagheri, *Sens. Actuators, B*, 2005, **107**, 53–58.
61 M. Shamsipur, T. Poursaberi, A. R. Karami, M. Hosseini, A. Momeni, N. Alizadeh, M. Yousefi and M. R. Ganjali, *Anal. Chim. Acta*, 2004, **501**, 55–60.
62 IUPAC, *Spectrochim. Acta, Part B*, 1978, **33**, 241–245.
63 O. Babaiah, C. K. Rao, T. S. Reddy and V. K. Reddy, *Talanta*, 1996, **43**, 551–558.
64 H. D. Gunawardhana, *Analyst*, 1983, **108**, 952–958.
65 R. L. Nunez, M. C. Mochon and A. G. Perez, *Talanta*, 1986, **33**, 587–591.
66 V. Vojković, V. A. Zivcić and V. Druskovic, *Spectrosc. Lett.*, 2004, **37**, 401–420.
67 Y. Yigzaw and B. S. Chandravanshi, *Microchim. Acta*, 1996, **124**, 81–87.
68 V. Srilalitha, A. R. G. Prasad, K. R. Kumar, V. Seshagiri and L. R. K. R. Ravindranath, *Facta Univ., Ser.: Phys., Chem. Technol.*, 2010, **8**, 15–24.
69 D.-J. Wang, J.-Y. Zhuang, Z.-H. Xie, Q.-Q. Fan, Z.-X. Zhang and W.-J. Chai, *Microchim. Acta*, 1992, **108**, 79–91.
70 P. K. Tarafder and R. Thakur, *Talanta*, 2008, **75**, 326–331.
71 R. K. Mondal and P. K. Tarafder, *Microchim. Acta*, 2004, **148**, 327–333.
72 B. Tamhina and V. Vojković, *Microchim. Acta*, 1986, **88**, 135–145.
73 H. P. Tarasiewicz, M. Tarasiewicz and W. Misiuk, *Microchem. J.*, 1984, **29**, 341–344.
74 N. Baccan, *Fresenius' Z. Anal. Chem.*, 1983, **316**, 796–799.
75 A. S. Amin and Z. Al-Malah, *J. Ind. Environ. Chem.*, 2017, **1**, 33–40.
76 J. N. Miller and J. C. Miller, *Statistics and Chemometrics for Analytical Chemistry*, Prentice Hall, England, 2005.